



CHORUS

This is the accepted manuscript made available via CHORUS. The article has been published as:

Underwater Restoration and Retention of Gases on Superhydrophobic Surfaces for Drag Reduction

Choongyeop Lee and Chang-Jin Kim

Phys. Rev. Lett. **106**, 014502 — Published 7 January 2011

DOI: [10.1103/PhysRevLett.106.014502](https://doi.org/10.1103/PhysRevLett.106.014502)

Underwater gas restoration and retention on superhydrophobic surfaces for drag reduction

Choongyeop Lee and Chang-Jin "CJ" Kim

Mechanical and Aerospace Engineering Department

University of California, Los Angeles (UCLA), California 90095, U.S.A.

Superhydrophobic (SHPo) surfaces have shown promise for passive drag reduction because their surface structures can hold a lubricating gas film between the solid surface and the liquid in contact with it. However, the types of SHPo surfaces that would produce any meaningful amount of reduction get wet under liquid pressure or at surface defects, both of which are unavoidable in real world. In this report, we solve the above problem by (1) discovering surface structures that allow the restoration of a gas blanket from a wetted state while fully immersed underwater and (2) devising a self-controlled gas generation mechanism that maintains the SHPo condition under high liquid pressures (tested up to 7 atm) as well as in the presence of surface defects, thus removing a fundamental barrier against the implementation of SHPo surfaces for drag reduction.

47.85.lb, 68.08.Bc, 81.40.Pq, 83.50.Rp

Recently, structured hydrophobic surfaces exhibiting superhydrophobicity have shown promise as gas-lubricated surfaces because their surface structures can hold a gas film when submerged in a liquid [1-8] (Fig. 1(a)). Some have even demonstrated

effective slip lengths [9] up to hundreds of micrometers [6,7], which are large enough to benefit regular (i.e., large) fluidic systems. Drag reduction for turbulent flows has also been reported [8]. SHPo surfaces are considered a superior alternative to the existing bubble injection method [10] for drag reduction, because the stable gas upon the surfaces makes the SHPo method passive (i.e., energy efficient) and simple (i.e., easy implementation). Moreover, it has been shown that the minimized solid-liquid contact on SHPo surfaces can resist surface fouling [11]. Despite its great potential, drag reduction by SHPo surfaces has been considered strictly limited to laboratory conditions because of one main unanswered question: can they retain the gas under real conditions? This problem is rather fundamental and should be addressed first, so that more practical issues like biofouling and cost are even relevant. Because the wetting transition of a SHPo surface is spontaneous, any liquid impregnation, incited by various instigators [12,13], has an irrevocable effect against drag reduction, as illustrated in Figs. 1(a)-1(c). For example, the surface may get wet and lose its slip effect if it has defects, the liquid is under pressure [12], or the gas diffuses away over time [13].

Recently, several approaches have been suggested to increase the stability of the gas layer on a SHPo surface against liquid pressure [7,14,15]: e.g., nanostructuring the sidewall of the microstructures [7] and pressurizing the gas layer [14,15]. However, these approaches are only preventive measures. They are ineffective once the gas layer is disrupted. More desirable is the ability to restore underwater superhydrophobicity even after the surface structures become wetted. A successful scheme should be able to displace the liquid that has impregnated the surface structures with new gas and reform a stable gas film, as illustrated in Fig. 1(d). Note the recovery of the SHPo state shown for

sessile droplets surrounded by air [16,17] is not helpful for drag reduction, which pertains to the entire surface being fully immersed underwater.

To restore a stable gas layer, we reason that the new gas should not grow vertically off the surface structures before spreading laterally between them. We propose that this goal can be achieved by designing the surface structures to satisfy a certain geometric criterion, given below for post structures (See supplementary material for details [18], which addresses the case of grate structures as well).

$$(\sqrt{2} - 2\sqrt{(1-\phi)/\pi}) \frac{-1 + \sin \theta_{p,adv}}{2 \cos \theta_{p,adv}} < H / L < \frac{-\cos \theta_{b,rec}}{2 \sin \theta_{p,rec} (1 - \sqrt{\pi(1-\phi)/\phi})} \quad (1)$$

where ϕ , H , L , θ are the gas fraction ($\phi = 1 - \pi D^2 / 4L^2$, D : diameter of posts), height and pitch (center-to-center distance) of the posts, and contact angle (CA), respectively. For the CA θ , the subscripts *adv* and *rec* mean advancing and receding, and subscripts p and b refer to the top surface of the posts and the bottom surface between the posts, all respectively. The upper bound value of H/L shown in Eq. (1) was derived from a geometric requirement that the gas should grow with less resistance in the lateral direction than in the vertical. The maximum gas pressure the interfaces can sustain against vertical (i.e., undesirable) growth is $\Delta P_v = (\gamma \pi D \sin \theta_{p,rec}) / L^2 \phi$, while the minimum pressure needed to sustain the lateral growth (i.e., the two vertical contact lines on the sidewall of a post merge and depart from the wall) is $\Delta P_l = (L \cos \theta_{b,rec} + 2H \sin \theta_{p,rec}) / HL$. The first and second term represent the resistance by the bottom surface and that by the post sidewall, respectively. For the bubble to grow laterally without vertical outgrowth, the gas pressure should be higher than ΔP_l but lower

than ΔP_v , providing a qualitative guideline for the design of SHPo surfaces that allow the restoration of a stable gas layer. The lower bound value of H/L in Eq. (1) was derived from another geometric requirement that, once the gas film is formed, the liquid-gas meniscus should not touch the bottom surface as a result of the liquid pressure, conditioning that the height of the posts should be greater than the maximum sagging depth of the meniscus [2].

When CA_{rec} on the bottom surface is 110° , corresponding to a smooth surface of a highly hydrophobic material (e.g., Teflon[®]), there is only a limited regime that satisfies the right side of Eq. (1) (Fig. 2(a)). In order to increase this $CA_{\text{b,rec}}$ further, expanding the regime of satisfactory values, we propose to nanostructure the bottom surface and render it a solid-gas composite. According to the Cassie-Baxter equation [19],

$$\cos \theta_c = \phi + (1 - \phi) \cos \theta \quad (2)$$

where θ is the intrinsic CA on a smooth surface and θ_c is the apparent CA on the nanostructured surface. $\theta = 110^\circ$, θ_c can be increased to 173.4° by employing nanostructures with a gas fraction of 0.99. Accordingly, the geometric regime of posts that satisfy Eq. (1) is significantly expanded if the bottom surface is nanostructured (Fig. 2(a)). This approach is schematically represented in Fig. 2(b). When the microstructures become wetted, a residual gas remains in between the nanostructures due to their high resistance against liquid impalement, keeping the bottom surface SHPo. When there is an influx of gas, the large contact angle on the SHPo bottom surface helps the gas spread past the posts laterally and recover the gas layer amongst the microstructures.

Based on the aforementioned geometrical requirements for successful gas spreading, hydrophobic microstructures were constructed on a substrate surface covered in hydrophobic nanostructures, as shown in Fig. 2(c). To fabricate such hierarchical SHPo surfaces, nanostructures were formed on a 4 inch silicon wafer using a black silicon method, on which a gas fraction over 99% and contact angle over 175° were reported previously [2]. After depositing and patterning Au (~ 200 nm) as electrodes for electrolysis on the bottom surface, 50 μm -thick negative photoresist (KMPR1050, Microchem) was spin-coated on the wafer, and microstructures (posts or grates) with varying pitches and gas fractions were patterned out of the photoresist. Finally, to make all the surfaces hydrophobic, 2 wt% Teflon[®] AF solution (Dupont) was spin-coated.

To replenish the gas layer lost upon wetting, electrolysis was deemed better suited than other gas-generation methods such as thermal, pneumatic, and chemical on account of its low power consumption [20], the stability of the generated gases [21], its easy integration into a system, and its compatibility with water. In this study, we used a line pattern of thin-film gold on the bottom surface as the cathode (Fig. 2(c)) and a copper wire in the water as the anode to perform electrolysis. The placement of the electrodes on the bottom surface imposes a self-controlled (i.e., self-activating and self-limiting) generation of gas, because the electrolytic circuit closes, starting gas generation, only when and where the microstructures become wetted (i.e., the liquid touches the cathode), and opens, halting the gas generation, as soon as the de-wetting is complete.

A series of experiments were conducted to verify the effectiveness of the proposed scheme by restoring underwater superhydrophobicity under the worst-case scenario of all the microstructures being wet. Before applying any voltage, the water tank was first

subjected to a moderate vacuum (1-2 kPa), which made all the microstructures wet but not the nanostructures. After the wetting was confirmed, we applied 10 V between the cathode on the sample and the anode wire 1 cm above the sample inside the water, starting electrolysis. As a reference, we prepared a control surface having microposts on a smooth bottom surface (Fig. 3(a)). In this case, the generated gas tended to produce several individual bubbles, which protruded over the top of the posts rather than forming a film, failing to cover the surface evenly (See video S1 in [18]). For the proposed surface having microposts on a nanostructured bottom (Figs. 3(b)-3(c)), in comparison, a non-wetted area was gradually recovered as the gas film spread without protruding over the microposts. The entire test area (2 cm x 2 cm) became de-wetted after several minutes (See videos S2-S3 in [18]). A schematic illustration of bubble generation on the wetted surface of microposts is shown in Fig. S6 in [18], along with the test setup.

A de-wetting process begins with patches of gas film appearing at random locations in a wetted area. After that, the growth of gas occurs mainly via Oswald ripening [22], since the gas is interconnected everywhere via the thin residual layer on the bottom surface between the nanostructures. In Oswald ripening, the gas inside the smaller bubbles is transported to the larger bubbles (i.e., a gas film) due to the difference in Laplace pressures, leading to the continuous growth of a large gas film until the gas film covers the whole area. The current approach was also applied to regenerate a gas layer on a surface of grating microstructures as well, as shown in Fig. 3(d) and video S4.

The total power consumption needed for complete restoration of the gas film on the test area of 2 cm by 2 cm was estimated to be about 6 mW for 150 sec. This value, while much larger than the inherent power requirement due to the Teflon layer covering the

electrodes and the accompanying components in the test setup, is nonetheless much smaller than that needed for a thermal method (e.g., 1-100 W [20]). It is worth noting that the presence of nanostructures on the bottom surface offers another advantage for practical applications. When a liquid impregnates microstructures on a smooth bottom surface, the wetting tends to spread rapidly to the surrounding area, leading to a cascade of wetting over the entire area [6]. In contrast, with the bottom surface nanostructured and superhydrophobic in its own right against liquid pressure, our surfaces confine the wetting to limited regions and resist further liquid spreading. This feature helps restore a gas layer on microstructures with surface defects [23].

Another important implication of our surface for practical applications is that our surface can retain a stable gas layer even under high liquid pressure. An electrolytically generated gas automatically adjusts its pressure to that of the liquid, such that a gas layer on our surface can effectively resist high liquid pressure. We experimentally verified that a gas layer can be retained on our surface under pressurized liquid (tested up to 7 atm) by employing the current gas restoration scheme. This feature can significantly expand the applicability of a SHPo surface to a number of practical applications involving high liquid pressure or biofouling. For example, the underwater pressure on the hull of most large ocean liners ranges up to 1-3 atm.

To confirm that the restoration of gas film indeed recovers the drag reduction, we measured slip lengths on microposts and microgrates (a circular test area of 6 cm in diameter) using a rheometer [6,24] with the current gas restoration scheme applied. To start, the slip lengths on non-wetted surfaces were measured to be consistent with theoretical values for grates [25,26] and posts [6,27] (“Never-wetted” in Fig. 4). After the

surfaces were wetted (by diffusing away the gas in the surface structures to the bulk water), the slip was lost (“Wetted” in Fig. 4), as expected. When gas films were restored on the surfaces by our electrolytic regeneration scheme, the slip lengths were found to approach the values obtained before the wetting, confirming that the regenerated gas layer is as effective as the original gas layer in inducing a liquid slip (“De-wetted in Fig. 4).

In summary, the presented approach achieves underwater drag reduction by forming hydrophobic microstructures (known for large slip) of a certain geometric criterion on a hydrophobic nanostructured surface (known for a high stability against the wetting) integrated with a measure for self-limiting electrolysis. By accommodating high liquid pressure and defective surfaces, this report opens the door to implement large-slip SHPo surfaces for real applications such as vessel surfaces and pipe flows.

This research has been funded by the NSF NIRT Program. The authors thank Prof. P. Kavehpour for access to the rheometer.

- [1] J. Ou, B. Perot and J. P. Rothstein, *Phys. Fluids* **16**, 4635 (2004).
- [2] C.-H. Choi and C.-J. Kim, *Phys. Rev. Lett.* **96**, 066001 (2006).
- [3] P. Joseph et al., *Phys. Rev. Lett.* **97**, 156104 (2006).
- [4] L. Bocquet and J.-L. Barat, *Soft Matter* **3**, 685 (2007).
- [5] P. Tsai et al., *Phys. Fluids* **21**, 112002 (2009).
- [6] C. Lee, C.-H. Choi and C.-J. Kim, *Phys. Rev. Lett.* **101**, 064501 (2008).
- [7] C. Lee and C.-J. Kim, *Langmuir* **25**, 12812 (2009).
- [8] J. P. Rothstein, *Annu. Rev. Fluid Mech.* **42**, 89 (2010).

[9] A slip length is defined as the virtual distance inside a solid surface at which a liquid velocity is extrapolated to zero. A slip length needs to be comparable to the length scale of the fluidic system (e.g., channel height, boundary layer thickness) for a meaningful amount of drag reduction.

[10] S. L. Ceccio, *Annu. Rev. Fluid Mech.* **42**, 183 (2010).

[11] A. J. Scardino, H. Zhang, D. J. Cookson, R. N. Lamb and R. de Nys, *Biofouling* **25**, 757 (2009).

[12] Q. S. Zheng, Y. Yu and Z. H. Zhao, *Langmuir* **21**, 12207 (2005).

[13] R. N. Govardhan, G. S. Srinivas, A. Asthana and M. S. Bobji, *Phys. Fluids* **21**, 052001 (2009).

[14] C. F. Carlborg, M. Do-Quang, G. Stemme, G. Amberg and W. van der Wijngaart, in *Proceedings of the 21st IEEE International Conference on Micro Electro Mechanical Systems* (IEEE, Tucson, 2008), p. 599.

[15] C. F. Carlborg, G. Stemme and W. van der Wijngaart, in *Proceedings of the 22nd IEEE International Conference on Micro Electro Mechanical Systems* (IEEE, Sorrento, 2009), p. 39.

[16] T. N. Krupenkin *et al.*, *Langmuir* **23**, 9128 (2007).

[17] J. B. Boreyko and C. H. Chen, *Phys. Rev. Lett.* **103**, 174502 (2009).

[18] See EPAPS Document for supplementary information.

[19] A. B. D. Cassie and D. Baxter, *Trans. Faraday Soc.* **40**, 546 (1944).

[20] D. D. Meng, Y. Ju and C.-J. Kim, in *Digest of Technical papers of the 13th International Conference on Solid-State Sensors, Actuators and Microsystems* (IEEE, Seoul, 2005), p. 1263.

- [21] C. Neagu, H. Jansen, H. Gardeniers and M. Elwenspoek, *Mechatronics* **10**, 571 (2000).
- [22] F.-M. Chang, Y.-J. Sheng, S.-L. Cheng and H.-K. Tsao, *Appl. Phys. Lett.* **92**, 264102 (2008).
- [23] In the presence of defects on microposts (i.e., missing posts), a wetted region was confined inside the defective area without propagating to the surrounding area, which was subsequently converted to be non-wetted by regenerated gases.
- [24] C.-H. Choi and C.-J. Kim, *Phys. Rev. Lett.* **97**, 109602 (2006).
- [25] E. Lauga and H. Stone, *J. Fluid Mech.* **489**, 55 (2003).
- [26] A. V. Belyaev and O. I. Vinogradova, *J. Fluid Mech.*, 652, 489 (2010).
- [27] C. Ybert, C. Barentine, C. Cottin-Bizonne, P. Joseph and L. Bocquet, *Phys. Fluids* **19**, 123601 (2007).

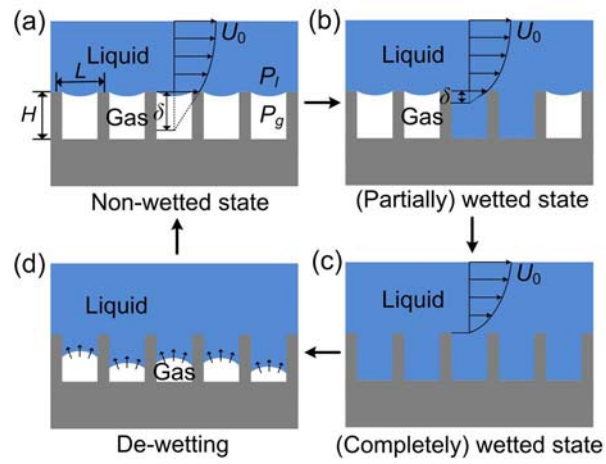


FIG. 1. Loss of slip by wetting transition and a hypothetical scenario to restore underwater superhydrophobicity.

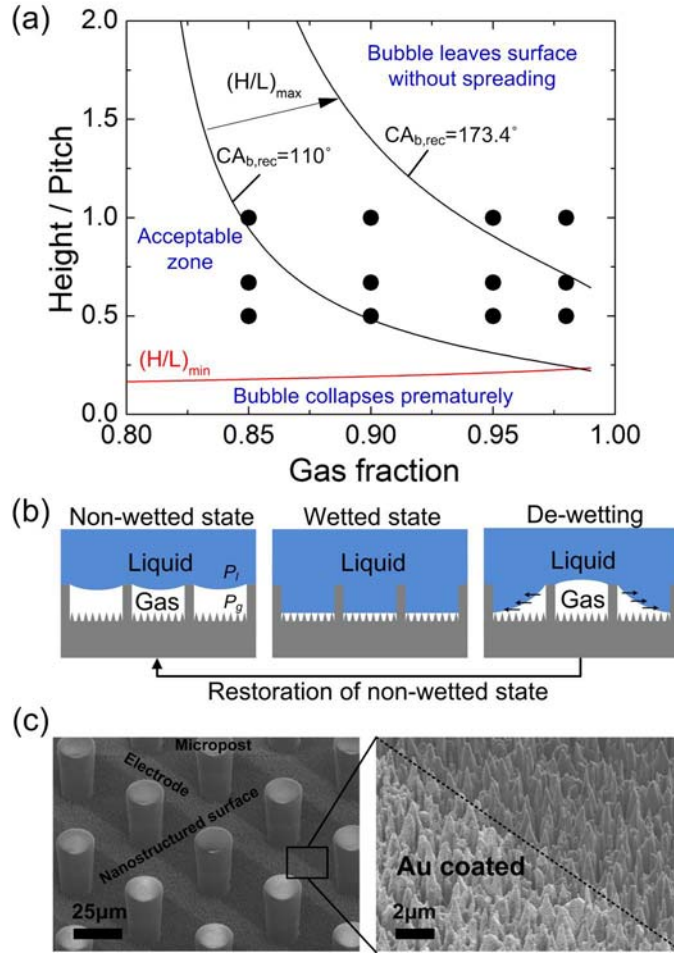


FIG. 2. Proposed scheme to restore gas film underwater, shown for micropost. (a) Estimated range of height-to-pitch ratio (H/L) that allows formation of a gas film between posts as function of their gas fraction with $CA_{b,rec}$ as a parameter. Red line represents the minimum H/L and black line the maximum H/L acceptable, following Eq. (1). Microposts of varying gas fraction and pitch (while height is fixed at $50\ \mu m$), denoted as “•” symbols, have been fabricated on both smooth and nanostructured bottom surfaces and tested. The gas film restoration was achieved only when the acceptable zone was expanded due to the increased CA_{rec} on the

nanostructured bottom surface, qualitatively agreeing with the theory. (b) Schematic representation of the successful gas film formation. (c) SEM images of a test surface fabricated based on the above criteria.

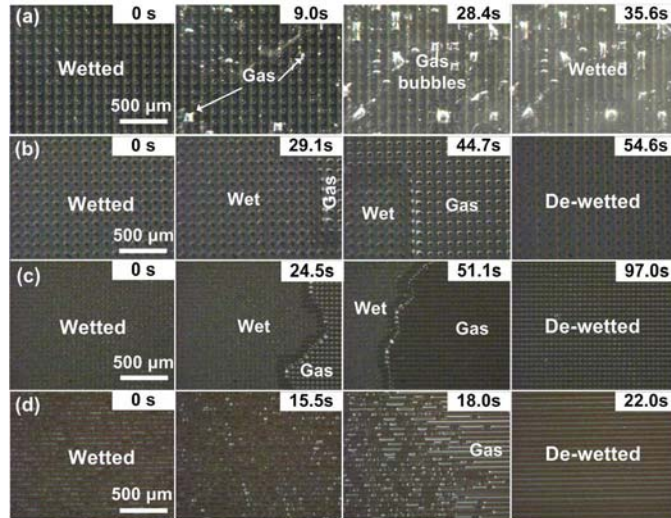


FIG. 3. Demonstration of restoration of underwater superhydrophobicity. (a) Gas generation on microposts (100 μm pitch, 50 μm height, 95% gas fraction) with the smooth bottom surface. (b-c) Gas generation on microposts (100 μm pitch for (b) and 50 μm pitch for (c), both 50 μm height and 95% gas fraction) with the nanostructured bottom surface. (d) Gas generation on microgrates (50 μm pitch, 50 μm height, 80% gas fraction) with the nanostructured bottom surface.

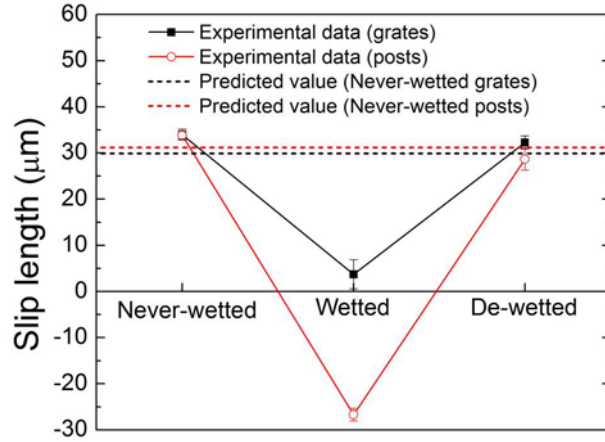


FIG. 4. Slip measurements with intentional wetting and active de-wetting underwater. Samples are a grid array of microposts (50 μm pitch, 90% gas fraction) and a concentric array of microgrates (80 μm pitch, 80% gas fraction), tested in succession: never-wetted (voltage on), wetted (voltage off), and de-wetted (voltage on). Each error bar represents the standard deviation of five data points.